

Gaia Calibrated UV Luminous Stars in LAMOST

Yu Bai¹, JiFeng Liu^{1,2}, Song Wang¹

¹ Key Laboratory of Optical Astronomy, National Astronomical Observatories, Chinese Academy of Sciences, 20A Datun Road, Chaoyang District, Beijing 100012, China; *ybai@nao.cas.cn*

² College of Astronomy and Space Sciences, University of Chinese Academy of Sciences, Beijing 100049, China Received 20XX Month Day; accepted 20XX Month Day

Abstract We take advantage of the Gaia data release 2 to present 275 and 1,774 ultraviolet luminous stars in the FUV and the NUV. These stars are 5σ exceeding the centers of the reference frame that is built with over one million UV stars in the $\log g$ vs T_{eff} diagram. The Galactic extinction is corrected with the 3D dusty map. In order to limit the Lutz-Kelker effect to an insignificant level, we select the stars with the relative uncertainties of the luminosity less than 40% and the trigonometric parallaxes less than 20%. We cross-identified our sample with the catalogs of RR Lyr stars and possible white dwarf main-sequence binaries, and find they compose $\sim 62\%$ and $\sim 16\%$ of our sample in the FUV and NUV, respectively. This catalog provides a unique sample to study stellar activity, spectrally unresolved compact main-sequence binaries and variable stars.

Key words: stars: activity — stars: general — ultraviolet: stars

1 INTRODUCTION

The majority of the stars in our Galaxy is cool, emitting much of the stellar electromagnetic radiation in the visible or near-infrared part of the spectrum. These cool stars are defined by the effective temperatures that are the thermal temperatures estimated from stellar photospheres. The higher regions of the stellar atmosphere (chromosphere, transition region, and corona) are often dominated by more violent non-thermal physical processes mainly powered by the magnetic field (Bai et al., 2018). These processes could produce high energy emissions in the UV or X-ray part of the spectrum, which are known as stellar activity.

The stellar activity could release a total energy higher than 10^{34} ergs, which leads to discrepancies between observations and the stellar theoretical models. Such discrepancy is severe in the UV band that is particularly sensitive to hot plasma emission ($\sim 10^4$ – 10^6 K). Therefore, the UV domain is ideal for investigating stellar activity, and its availability has been explored for Sun-like stars (Findeisen et al., 2011) and M dwarfs (Jones & West, 2016). An observational reference frame in the UV is essential to characterize the stellar activity and further to identify the truly peculiar stars, which is still poorly understood due to the

The UV luminous stars are outliers that don't fit such UV reference frame. They are probably flaring stars due to magnetic reconnection. The stellar magnetic field is thought to be generated and maintained by a stellar dynamo (Wright et al., 2011), or interaction in a binary star (Simon et al., 1980) or in a star-planets system (Ip et al., 2004). They could also be the stars with very hot atmospheres, e.g., accreting pre-main sequence stars (Eaton & Herbst, 1995), hot subdwarfs (Wang et al., 2017) and variable stars (Sesar et al., 2010; Bai et al., 2018). The excessive UV emission may be originated from the spectrally unresolved companions that are active late-type stars (Yang et al., 2017).

On the other hand, the main-sequence stars around compact objects that cannot be resolved by the LAMOST spectra, could also emit excessive UV photons (Jao et al., 2014). Such UV emission could be originated from the accretion disks round white dwarfs (Gänsicke et al., 1997, 2001), neutron stars or black holes. The ratios between X-ray and UV luminosity are about 0.1-100 for quiescent accretion disks around neutron stars and black holes (Hynes & Robinson, 2012; Cackett et al., 2013; Froning et al., 2014). This UV emission can provide important information to study compact objects in binary systems. Therefore, these UV outliers give us an unique sample that enables us to further investigate the stellar activity and the evolution of stars and binaries.

Bai et al. (2018) presented a UV catalog of over three million stars selected from the data release 3 of the LAMOST survey (Cui et al., 2012), in which about two third were detected by the *Galaxy Evolution Explorer* (*GALEX*; Morrissey et al. 2007). We take advantage of the catalog to study the UV reference frame with the help of the Gaia data release two (DR2; Gaia Collaboration et al. 2016, 2018a). We present the data for the calculation of UV luminosity in Section 2. The selection of the UV luminous stars is presented in Section 3. Section 4 gives a summary.

2 DATA

We calculate the average visit magnitudes in Bai et al. (2018) and extract the stellar parameters of the effective temperature (T_{eff}) and the surface gravity ($\log g$). Gaia DR2 provides parallaxes that can be used to obtain distance information. The UV stars are cross-matched to the Gaia DR2 with a match radius of $2''$. Estimating distance directly from the trigonometric parallax may suffer the Lutz–Kelker Effect (LKE), which was discussed in detail by Trumpler & Weaver (1953), and then parametrically formalized by Lutz & Kelker (1973). The effect is defined as an offset between the average absolute magnitudes for classes of stars as determined from trigonometric parallax samples and the true mean absolute magnitude for that stellar class (Lutz & Kelker, 1973; Sandage et al., 2016). The bias is found to be significant for stars with relative high parallax uncertainty, $\sigma_{\pi}/\pi \gtrsim 20\%$. However, the universal application of the correction for the bias has been challenged in more recent years (Smith, 2003; van Leeuwen, 2007; Francis, 2014). In order to limit the LKE to an insignificant level, we select the stars with relatively small uncertainties of the trigonometric parallaxes.

The Bayesian method developed by Burnett & Binney (2010) and Binney et al. (2014) has been used for stars in the RAVE survey, which has demonstrated the ability to obtain accurate distance and extinction. Wang et al. (2016) measured extinctions and distances using this method for stars with valid stellar parame-

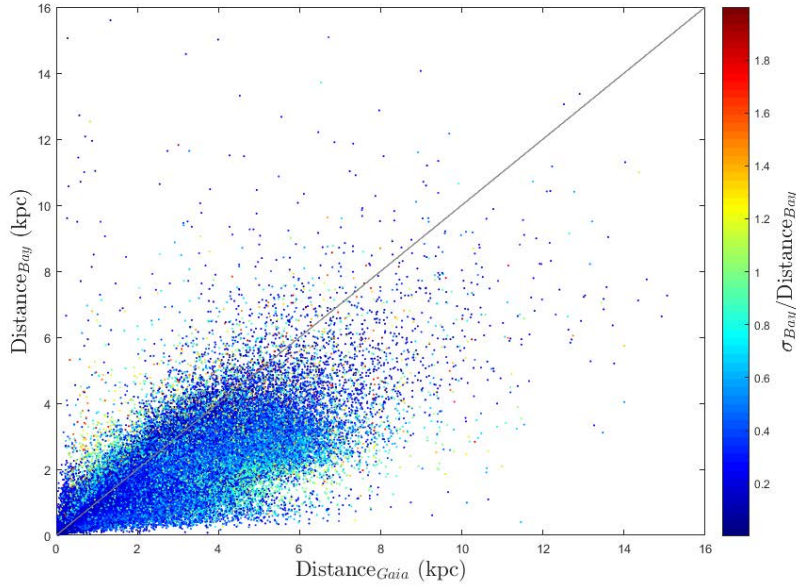


Figure 1: Comparison of distances estimated with the Bayesian method with those from Gaia. The color bar stands for the relative uncertainties of the Bayesian distances.

and $\log g$, and 2MASS photometry to compute the posterior probability with the Bayesian method. We compare their distances to those from Gaia in Fig. 1. Here, we plot the stars with relative uncertainties less than 20% for the Gaia distances, and don't constrain the relative uncertainties of the Bayesian distances (Bai et al., 2018). The distances from the Bayesian method are underestimated probably due to the uncertainties in the stellar parameters, if they are not well constrained in the LAMOST pipeline (Wu et al., 2011). The trigonometric parallaxes in the Gaia DR2, however, have good consistency with those from other methods (Gaia Collaboration et al., 2018b).

Galactic extinction plays a much larger role for the FUV/NUV than the other bands (Cardelli et al., 1989). In order to correct the extinction, we use the 3D dust map from Green et al. (2015), which gives $E(B-V)$ as a function of the distance and the position. In conjunction with Gaia parallax derived distances, we estimate the reddening in the line of sight for each star in our sample. We adopt the extinction coefficients from Yuan et al. (2013) and Jordi et al. (2010) for the FUV/NUV and Gaia bands, respectively. All the magnitudes presented hereafter are extinction-corrected. The HR diagram of our sample (Fig. 2, left panels) contains 1,474,479 UV stars with valid distances and extinctions, in which the magnitudes and colors are extracted from the Gaia DR2.

Using the trigonometric parallax from the Gaia DR2, we calculate the luminosity in the FUV/NUV. We select the stars with the relative uncertainty of L_{UV} less than 40%, and find that their $\sigma_{\pi}/\pi < 20\%$. In this case, the LKE in our sample does not significantly influence the luminosity. There are 85,444 and 1,271,863 stars satisfied the criteria in the FUV and NUV, respectively (Fig. 2, right panel). The number of stars with $M_G < -2$ are less than those in the full sample; this may be due to the LKE in which the absolute magnitudes are over estimated. We present the HR-like diagram of these stars in the Fig. 3. The stars become luminous with increasing effective temperatures, which is similar to the results of Shkolnik

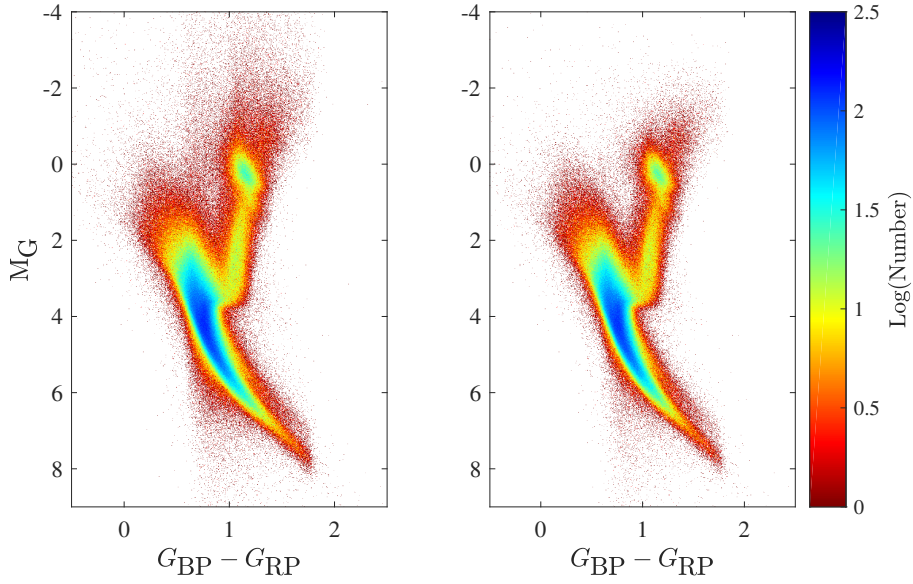


Figure 2: M_G vs $G_{BP} - G_{RP}$ distribution for the full UV star sample (left panel) and for the stars with the relative uncertainty of L_{UV} less than 40% (right panel). The color bar stands for the density in log scale.

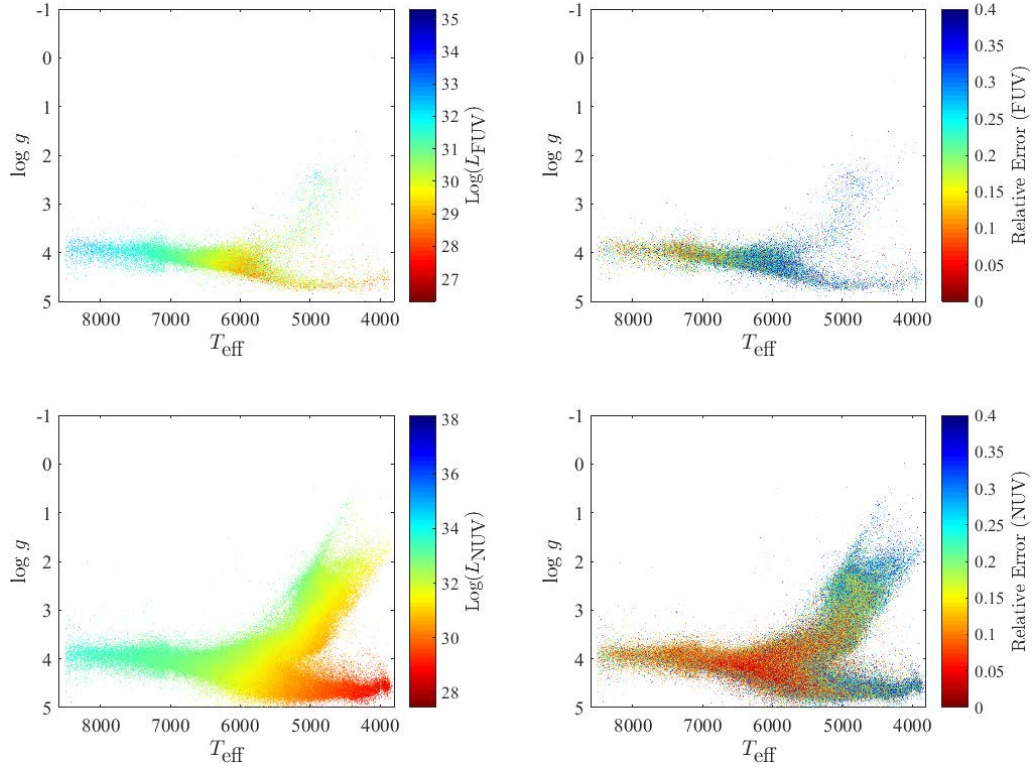


Figure 3: HR-like diagrams. The color bars stand for the luminosities in the FUV and NUV in the left two panels and the relative uncertainties of the luminosities in the right two panels.

3 RESULT

3.1 UV luminous stars

This luminosity catalog provides a wealth of information for the study of stellar UV emission, and enables

Table 1: Fit Result in the FUV.

Ind	T_{eff}	$\log g$	σ	μ	Num	HighNum	LowNum
(1)	(2)	(3)	(4)	(5)	(6)	(7)	(8)
1	4250	4.75	1.11±0.11	29.30±0.10	205	0	0
2	4350	4.75	0.77±0.06	29.29±0.06	243	0	0
3	4450	4.75	0.84±0.09	29.51±0.08	245	0	0
4	4550	4.75	0.95±0.06	29.59±0.06	243	0	0
5	4650	4.75	0.78±0.06	29.64±0.06	312	0	0
6	4750	2.75	0.75±0.07	31.07±0.07	260	0	0
7	4750	4.75	0.69±0.08	29.52±0.08	337	0	0
8	4850	2.75	0.69±0.06	31.23±0.06	253	0	0
9	4850	4.75	0.71±0.03	29.73±0.03	372	0	0
10	4950	2.75	0.76±0.04	31.23±0.04	200	0	0
11	4950	3.25	0.71±0.08	30.79±0.08	216	0	0
12	4950	4.75	0.77±0.04	29.74±0.04	440	0	0
13	5050	3.25	0.70±0.03	30.86±0.03	226	0	1
14	5050	3.75	0.74±0.04	30.48±0.04	212	0	0

(1). The index of the bin. (2). The median T_{eff} in the unit of K. (3). The median $\log g$. (4). The standard deviation of the Gaussian fit in erg s^{-1} . (5). The center of the distribution from the Gaussian fit in erg s^{-1} . (6). The number of stars in the bin. (7). The number of stars with the lower limit of luminosity 5σ higher than the center of the Gaussian fit. (8). The number of stars with the higher limit of luminosity 5σ lower than the center of the Gaussian fit.

(This table is available in its entirety in electric form.)

in $\log g$ and 100 K in T_{eff} . The distribution of the luminosity in each bin is fitted with a Gaussian function, if the number of the stars in the bin is more than 200. We then select the stars fall outside the normal ranges (5σ) of the Gaussian function. Here the σ stands for the standard deviation of the Gaussian fit. The fitting results are shown in Fig. 4, Table 1 and 2. The selection yields 275 luminous and 17 quiet stars in the FUV, and 1,774 luminous and 943 quiet stars in the NUV. The luminosity for these stars is listed in Table 3 and 4.

We plot the luminosity vs T_{eff} in the left panels of Fig. 5. The UV luminous and quiet stars are located along the main sequence, when $T_{\text{eff}} \gtrsim 5500$ K. For the stars with $T_{\text{eff}} \lesssim 5500$ K, since they are no longer dominated by dwarfs, the distributions for the UV luminous and quiet stars aren't located along the main sequence. We find that the UV quiet stars are consistent with the theoretical model (the contours in Fig. 5). These stars don't shown obvious UV excesses above the emission predicted by the model. The luminosity vs $F(N)UV - H$ is shown in the right panels in Fig. 5. The UV luminous and quiet stars don't distribute along the main sequence, because the UV - IR colors of the early type stars depend on the T_{eff} (Bai et al., 2018). Again, the color of the UV quiet stars are consistent with the theoretical colors from the model.

3.2 What are these stars?

RR Lyrae (RR Lyr) stars are pulsating periodic horizontal branch variables with great variation in the UV with a range of 2C5 mag (Wheatley et al., 2012), making them more likely to be strong UV emitters. We cross-match the UV luminous stars with the RR Lyr catalogs in Sesar et al. (2010), Drake et al. (2013),

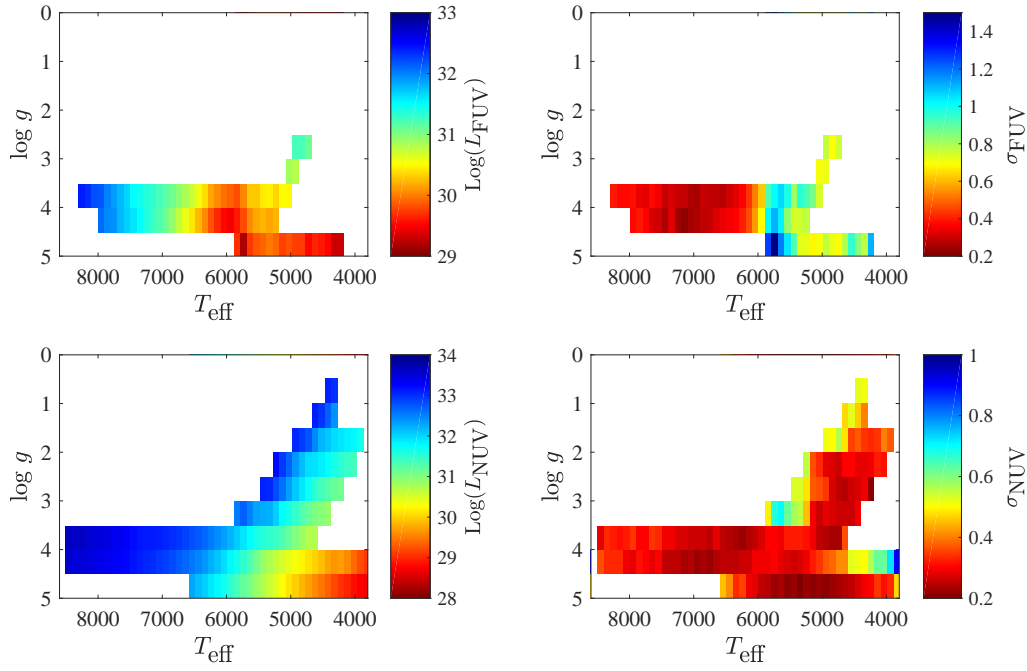


Figure 4: Distributions of the fit results in the FUV (left panel) and the NUV (right panel). The color bars stand for the μ and the σ for the Gaussian fit in the bins

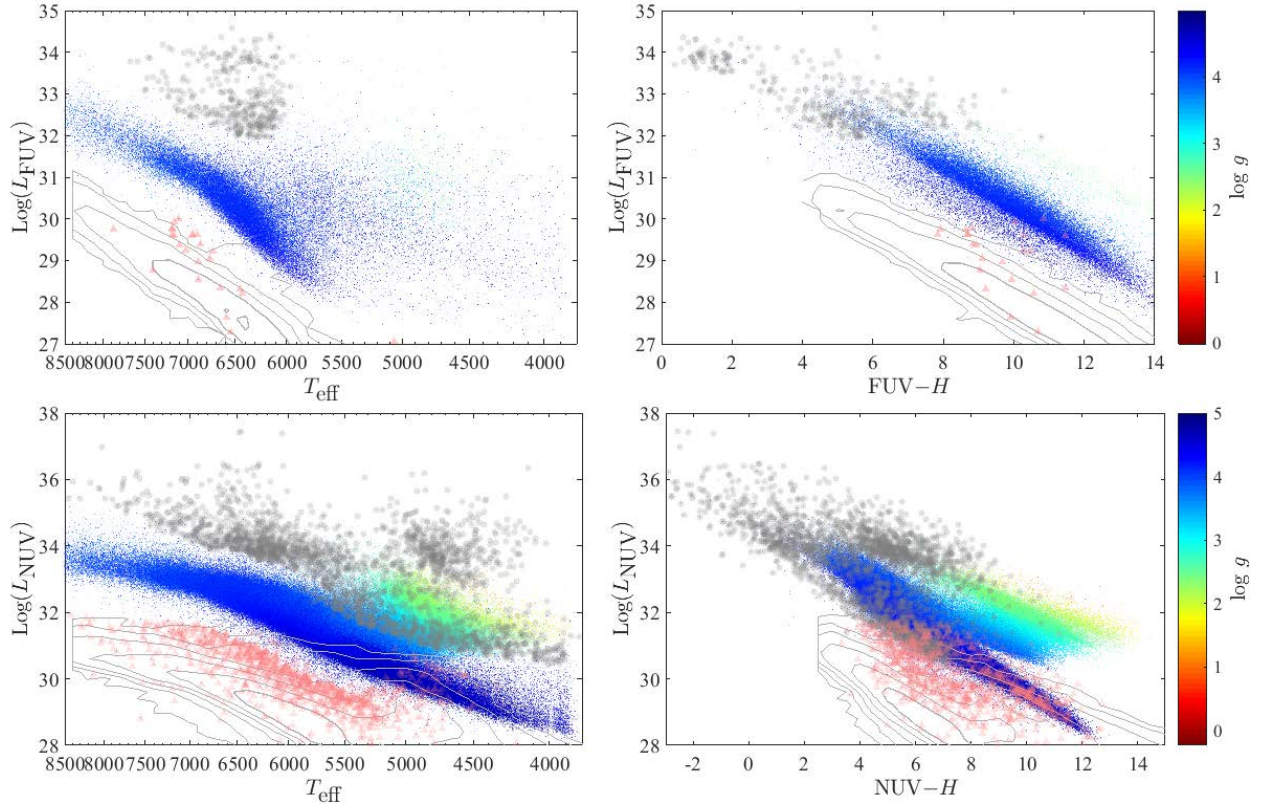


Figure 5: UV luminosity vs T_{eff} (left panels) and UV $-H$ color (right panels). The UV luminous stars are grey points, and the UV quiet stars are pink triangles. The contours stand for the distributions from the BT-Cond grid (Allard & Freytag, 2010) of the PHOENIX photospheric model (Hauschildt et al., 1999). The colorbars are the values of $\log g$.

Table 2: Fit Result in the NUV.

Ind	T_{eff}	$\log g$	σ	μ	Num	HighNum	LowNum
1	3850	4.25	0.90±0.10	29.07±0.09	247	0	0
2	3850	4.75	0.47±0.08	28.69±0.07	767	2	0
3	3950	1.75	0.37±0.03	31.63±0.03	397	0	0
4	3950	4.25	0.72±0.04	29.20±0.03	782	0	0
5	3950	4.75	0.33±0.03	28.73±0.03	1647	26	0
6	4050	1.75	0.40±0.03	31.78±0.03	570	2	0
7	4050	2.25	0.31±0.02	31.35±0.02	361	0	0
8	4050	4.25	0.62±0.05	29.37±0.05	529	0	0
9	4050	4.75	0.31±0.03	28.82±0.03	1939	28	0
10	4150	1.75	0.34±0.02	31.83±0.02	677	1	0
11	4150	2.25	0.32±0.02	31.42±0.02	796	3	0
12	4150	4.25	0.62±0.05	29.56±0.05	394	0	0
13	4150	4.75	0.34±0.02	28.95±0.02	2640	18	0
14	4250	1.75	0.33±0.02	31.89±0.02	778	3	1

The same to Table 1 but in the NUV

(This table is available in its entirety in electric form.)

Table 3: The FUV luminous and quiet stars.

Ind	Obsid	$\log(L_{\text{FUV}})$	$\log(eL_{\text{FUV}})$	Flag	Type	Catalog	WDMS
(1)	(2)	(3)	(4)	(5)	(6)	(7)	(8)
13	55109124	27.07	26.65	0	Star		
41	128907057	32.86	32.20	1	Star		
42	133409048	33.28	32.48	1	RR	D	
42	231312031	32.76	32.26	1	RR	D	
43	260814117	34.40	33.48	1	Hot subdwarf		
44	31410196	32.65	32.13	1	RR	D	
44	75313026	32.53	32.07	1	RR		
44	145411088	32.50	31.92	1	RR	D	
44	148715114	32.65	32.12	1		D	
44	154611186	32.72	32.17	1	RR		
44	189215005	33.45	32.96	1	RR	D	
44	218501180	32.36	30.85	1	Star		1

(1). The index of the bin that the stars are located in. (2). The LAMOST obsid. (3). The luminosity in erg s^{-1} . (4). The uncertainty of the luminosity in erg s^{-1} . (5). The stars with the lower limit of luminosity higher than the center the Gaussian fit by 5σ , Flag = 1, and the stars with the higher limit of luminosity lower than the center by 5σ , Flag = 0. (6). The types from the Simbad archive data. (7). The catalog flag. 'D'– Drake et al. (2013), 'S'– Sesar et al. (2010), and 'A'– Abbas et al. (2014). (8). The flag of the WDMS candidates.

(This table is available in its entirety in electric form.)

stars that are luminous in the FUV and NUV, respectively. The chances to match a RR Lyr star are $\sim 17\%$ and $\sim 4\%$ in the FUV and NUV of our sample, higher than that in the UV star catalog, $\lesssim 0.1\%$ (Bai et al.,

Table 4: The NUV luminous and quiet stars.

Ind	Obsid	$\log(L_{\text{NUV}})$	$\log(eL_{\text{NUV}})$	Flag	Type	Catalog	WDMS
9	241109013	30.96	29.17	1	Binary		1
9	335113059	30.74	29.99	1	Star		1
19	318815093	27.92	27.34	0	High proper-motion Star		
30	267316208	33.62	33.01	1	Eclipsing binary of Algol type		
30	286203005	32.80	32.13	1			
30	269109099	29.77	29.21	0			
32	321511220	32.50	31.64	1	White Dwarf		1
40	210907122	30.86	29.42	1	X-ray source		1
111	217614072	34.19	33.76	1	RR	D	
121	151015067	33.65	32.89	1	RR	DA	

The same to Table 3 but in the NUV

(This table is available in its entirety in electric form.)

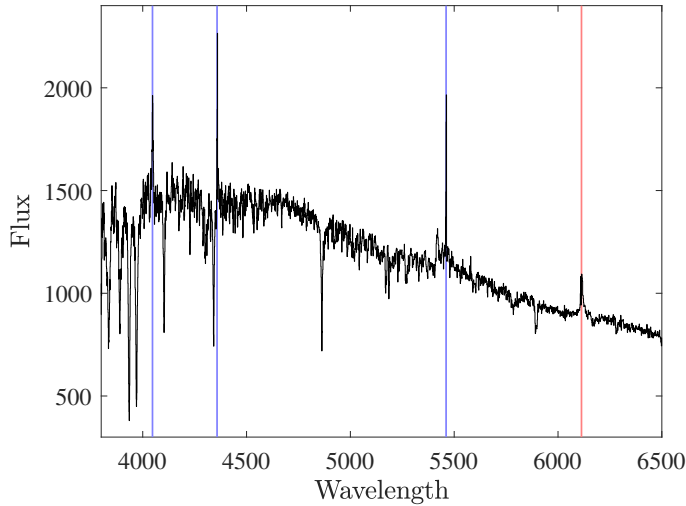


Figure 6: LAMOST spectrum of a UV luminous star (Obsid = 167801105). The red lines mark the Hg I emission lines, and the blue line is the Fe II emission line.

The binaries composed of non-degenerate stars and white dwarfs are probably unresolved by LAMOST spectra, and these binaries may become more luminous in the UV than that expected for the secondary stars. Bai et al. (2018) presented a sample of the potential white dwarf main-sequence binaries based on their density distribution in the FUV – NUV vs $W1 - W2$, which are extracted from *GALEX* and *WISE* catalogs. We cross-match the UV luminous stars with this sample, and find 123 and 213 stars in the FUV and NUV corresponding to $\sim 45\%$ and $\sim 12\%$ of our sample. If these stars are white dwarf binaries, their UV luminosities are dominated by the accretion disks or the hot atmospheres of the white dwarfs.

The FUV – NUV vs $W1 - W2$ diagram are powerful to select white dwarf plus M dwarf binaries, since their emissions are mainly in the UV and IR bands, respectively. For binaries with secondary stars with earlier than M, the IR color is not sensitive enough to distinguish white dwarf binaries from single stars. We present an example of a UV luminous star in Fig. 6. It is a spectrally identified F star with $T_{\text{eff}} = 6298$ K, and $\log g = 4.05$. Its FUV luminosity exceeds the center of the reference frame by 5.9σ . The three

II $\lambda 6113$ originated from hot thin gas, which has been detected in the nova spectra, e.g., Cyg 2014¹ and V445 Puppis (Iijima & Nakanishi, 2008). The star probably harbors in a binary system around a spectrally unresolved white dwarf that raises the FUV emission and the Fe II line. This implies that there are some potential white dwarf – G dwarf binaries and white dwarf – F dwarf binaries in our sample, which require additional optical colors to isolated them.

There may be also some active stars or active non-degenerate binaries in our sample. They are probably fast rotating stars with strong stellar activity (Reiners, 2012), or they may have the interconnecting field lines with the companion (Simon et al., 1980). They also could be very young stars or hot subdwarfs with UV excessive emission from hot atmospheres. The neutron star and the black hole binaries aren't ruled out, but we need multi-band information from radio to X ray to identify them.

4 SUMMARY

We present a catalog of 275 and 1,774 luminous stars in the FUV and NUV, which exceed the center of the local reference frame with at least 5σ . The reference frame is built with over one million LAMOST UV stars in $\log g$ vs T_{eff} diagram. We correct the extinction for the UV emission using the 3D dusty map with the distances from the Gaia DR2. These UV luminous stars are selected with the relative uncertainties of the luminosity less than 40% and the trigonometric parallax less than 20%, therefore they don't suffer significant LKE. We cross-match our sample with the catalogs of RR Lyr stars and possible white dwarf main-sequence binaries, and they in all compose $\sim 62\%$ and $\sim 16\%$ of our sample in the FUV and NUV, respectively.

This catalog provides an ideal sample to study stellar activity, compact main-sequence binaries and variable stars. These objects probably have optical spectra similar to normal stars, but have abnormal emission in the UV. We are going to use the most recent data release of the LAMOST to enlarge the sample, and study them in detail to further shed light on the nature of these UV luminous stars.

Acknowledgements This work was supported by the National Program on Key Research and Development Project (Grant No. 2016YFA0400804) and the National Natural Science Foundation of China (NSFC) through grants NSFC-11603038/11333004/11425313/11403056. Some of the data presented in this paper were obtained from the Mikulski Archive for Space Telescopes (MAST). STScI is operated by the Association of Universities for Research in Astronomy, Inc., under NASA contract NAS5-26555. Support for MAST for non-HST data is provided by the NASA Office of Space Science via grant NNX09AF08G and by other grants and contracts.

The Guoshoujing Telescope (the Large Sky Area Multi-Object Fiber Spectroscopic Telescope, LAMOST) is a National Major Scientific Project which is built by the Chinese Academy of Sciences, funded by the National Development and Reform Commission, and operated and managed by the National Astronomical Observatories, Chinese Academy of Sciences.

This work has made use of data from the European Space Agency (ESA) mission *Gaia* (<https://www.cosmos.esa.int/gaia>), processed by the *Gaia* Data Processing and Analysis Consortium (DPAC, <https://www.cosmos.esa.int/web/gaia/dpac/consortium>). Funding for the

DPAC has been provided by national institutions, in particular the institutions participating in the *Gaia* Multilateral Agreement.

References

- Abbas, M. A., Grebel, E. K., Martin, N. F., et al. 2014, *MNRAS*, 441, 1230
- Allard, F., & Freytag, B. 2010, *Highlights of Astronomy*, 15, 756
- Bai, Y., Liu, J., Wicker, J., et al. 2018, *ApJS*, 235, 16
- Binney, J., Burnett, B., Kordopatis, G., et al. 2014, *MNRAS*, 437, 351
- Burnett, B., & Binney, J. 2010, *MNRAS*, 407, 339
- Cackett, E. M., Brown, E. F., Degenaar, N., et al. 2013, *MNRAS*, 433, 1362
- Cardelli, J. A., Clayton, G. C., & Mathis, J. S. 1989, *ApJ*, 345, 245
- Cui, X.-Q., Zhao, Y.-H., Chu, Y.-Q., et al. 2012, *Research in Astronomy and Astrophysics*, 12, 1197
- Drake, A. J., Catelan, M., Djorgovski, S. G., et al. 2013, *ApJ*, 765, 154
- Eaton, N. L., & Herbst, W. 1995, *AJ*, 110, 2369
- Froning, C. S., Maccarone, T. J., France, K., et al. 2014, *ApJ*, 780, 48
- Findeisen, K., Hillenbrand, L., & Soderblom, D. 2011, *AJ*, 142, 23
- Francis, C. 2014, *MNRAS*, 444, L6
- Gaia Collaboration, Prusti, T., de Bruijne, J. H. J., et al. 2016, *A&A*, 595, A1
- Gaia Collaboration, Brown, A. G. A., Vallenari, A., et al. 2018, arXiv:1804.09365
- Gaia Collaboration, Babusiaux, C., van Leeuwen, F., et al. 2018, arXiv:1804.09378
- Gänsicke, B. T., Beuermann, K., & Thomas, H.-C. 1997, *MNRAS*, 289, 388
- Gänsicke, B. T., Szkody, P., Sion, E. M., et al. 2001, *A&A*, 374, 656
- Green, G. M., Schlafly, E. F., Finkbeiner, D. P., et al. 2015, *ApJ*, 810, 25
- Hauschildt, P. H., Allard, F., & Baron, E. 1999, *ApJ*, 512, 377
- Hynes, R. I., & Robinson, E. L. 2012, *ApJ*, 749, 3
- Iijima, T., & Nakanishi, H. 2008, *A&A*, 482, 865
- Ip, W.-H., Kopp, A., & Hu, J.-H. 2004, *ApJ*, 602, L53
- Jao, W.-C., Henry, T. J., Subasavage, J. P., et al. 2014, *AJ*, 147, 21
- Jordi, C., Gebran, M., Carrasco, J. M., et al. 2010, *A&A*, 523, A48
- Jones, D. O., & West, A. A. 2016, *ApJ*, 817, 1
- Lutz, T. E., & Kelker, D. H. 1973, *PASP*, 85, 573
- Morrissey, P., Conrow, T., Barlow, T. A., et al. 2007, *ApJS*, 173, 682
- Reiners, A. 2012, *Living Reviews in Solar Physics*, 9, 1
- Sandage, A., Beaton, R. L., & Majewski, S. R. 2016, *PASP*, 128, 064202
- Sesar, B., Ivezić, Ž., Grammer, S. H., et al. 2010, *ApJ*, 708, 717
- Shkolnik, E. L. 2013, *ApJ*, 766, 9
- Simon, T., Linsky, J. L., & Schiffer, F. H., III 1980, *ApJ*, 239, 911

- Trumpler, R. J., & Weaver, H. F. 1953, *Dover Books on Astronomy and Space Topics*, New York: Dover Publications
- van Leeuwen, F. 2007, *Astrophysics and Space Science Library*, 350
- Wang, J., Shi, J., Pan, K., et al. 2016, *MNRAS*, 460, 3179
- Wang, L., Gies, D. R., & Peters, G. J. 2017, *ApJ*, 843, 60
- Wheatley, J., Welsh, B. Y., & Browne, S. E. 2012, *PASP*, 124, 552
- Wright, N. J., Drake, J. J., Mamajek, E. E., & Henry, G. W. 2011, *ApJ*, 743, 48
- Wu, Y., Luo, A.-L., Li, H.-N., et al. 2011, *Research in Astronomy and Astrophysics*, 11, 924
- Yang, H., Liu, J., Gao, Q., et al. 2017, *ApJ*, 849, 36
- Yuan, H. B., Liu, X. W., & Xiang, M. S. 2013, *MNRAS*, 430, 2188